

Hydrodynamical analysis of hadronic spectra in the 130 GeV /nucleon Au+Au collisions

Tetsufumi Hirano,¹ Kenji Morita,² Shin Muroya,³ and Chiho Nonaka⁴

¹Physics Department, University of Tokyo, Tokyo 113-0033, Japan

²Department of Physics, Waseda University, Tokyo 169-8555, Japan

³Tokuyama Womxn's College, Tokuyama, Yamaguchi 745-8511, Japan

⁴IMC, Hiroshima University, Higashihiroshima, Hiroshima, 739-8521, Japan

(Dated: May 21, 2019)

We study one-particle spectra and a two-particle correlation function in the 130 GeV /nucleon Au+Au collisions at RHIC by making use of a hydrodynamical model. We calculate the one-particle hadronic spectra and present the first analysis of Bose-Einstein correlation functions based on the numerical solution of the hydrodynamical equations which takes both longitudinal and transverse expansion into account appropriately. The hydrodynamical model provides excellent agreement with the experimental data in the pseudorapidity and the transverse momentum spectra of charged hadrons, the rapidity dependence of anti-proton to proton ratio and the pion Bose-Einstein correlation functions. Our numerical solution suggests the formation of the quark-gluon plasma with large volume and low net-baryon density.

PACS numbers: 24.10.Nz, 12.38.Mh, 25.75.Gz

Relativistic heavy ion collisions are one of the most attracting problems because they provide us chances to explore the nature of hot and dense hadronic matter which exists in the early universe [1]. Creation of a new state of matter, the quark-gluon plasma (QGP), and many other new phenomena are expected to be found in the Relativistic Heavy Ion Collider (RHIC) experiment at BNL of which the collision energy is much higher than any other accelerator. However, the complicated processes during them any-body interactions and multiparticle productions are quite hard to catch clear. Therefore, a simple phenomenological description is indispensable for the better understanding of the phenomena. The aims of this paper are, based on a hydrodynamical model, to draw a simple and clear picture of the space-time evolution of the hot and dense matter produced in the high energy heavy ion collisions at RHIC and to give a possible explanation for the recent experimental results.

We use a (3+1)-dimensional hydrodynamical model [2] to describe the space-time evolution by assuming the local thermal and chemical equilibrium. Some authors have already discussed RHIC results based on hydrodynamical models. Kolb et al. [3] discussed anisotropic flow by making use of a (2+1)-dimensional hydrodynamical model in which Bjorken's ansatz [4] was used for the beam direction. Hence, their discussion is limited only in the midrapidity region. Zschiesche et al. [5] also discussed HBT radii based on a hydrodynamical model in which the Bjorken's ansatz is used. Their analysis is concentrated on the effect of equation of state on the HBT radii rather than the comparison with experiment. One of the authors, T.H. have already reproduced the both the pseudorapidity and the transverse momentum spectra of

hadrons by using a full (3+1)-dimensional hydrodynamical model in Ref. [6], where main theme of the analysis is also anisotropic flow. In this paper, we focus our discussion on central collisions by assuming the cylindrical symmetry of the system. We calculate the one-particle hadronic spectra and present the first analysis of Bose-Einstein correlation functions based on the numerical solution of the hydrodynamical equations which takes both longitudinal and transverse expansion into account appropriately [2].

The hydrodynamical equations are given as

$$\partial_t T(x) = 0; \quad (1)$$

with the baryon number conservation law,

$$\partial_t (n_B(x)U(x)) = 0; \quad (2)$$

We numerically solved the above coupled equations for the perfect fluid by the method described in Ref. [2]. As for an equation of state (EOS), we adopt a bag model EOS in which phase transition of first order takes place [7]. The QGP phase is a free gas with bag constant B. The gas consists of massless quarks of three flavor and gluons. On the other hand, the hadronic phase is a free resonance gas with an excluded volume correction in which heavy resonances up to 2 GeV/c² of mass are included. These two phases are connected by the condition of pressure continuity. We show the pressure as a function of temperature and baryon chemical potential in Fig. 1. See Ref. [7] for the further detail. Putting the initial time as $t = 1.0 \text{ fm}/c$, we parameterize the initial energy density distribution and net baryon number distribution as simple gaussian forms (Fig. 2) [2]¹. The parameters in the model should be chosen so that calculated

Electronic address: morita@hep.phys.waseda.ac.jp

¹ In Ref. [2], gaussian parameterizations are applied to temperature

single-particle spectra reproduce the experimental results of Au+Au central collisions in the 130 GeV/nucleon at RHIC. The parameter set is summarized in Table I. Note that we use Bjorken's solution [4] only as an initial condition for the longitudinal flow velocity. Initial transverse flow is neglected. Once the freeze-out hypersurface is fixed, one can calculate the single particle spectra via Cooper-Frye formula [8]. We assume the bulk component dominates the freeze-out hypersurface, i.e., we put $k_d' = k_d$, for simplicity.² We take hadrons from decay of heavy resonances into account as well as directly emitted particles from the freeze-out hypersurface. The heavy resonances are also assumed to be emitted from the freeze-out hypersurface. We include decay processes $\pi^+ \rightarrow 2\pi^+ \pi^0$, $\pi^+ \rightarrow 3\pi^+ \pi^-$, $K^+ \rightarrow 3\pi^+ \pi^- \pi^0$, and $K^+ \rightarrow N\pi^+$. For the method of calculation, see Ref. [14, 15]. Figure 3 shows pseudorapidity distribution of charged hadrons. Preliminary experimental data are from the PHOBOS Collaboration [16]. Our result quite agrees well with the experimental data. Figure 4 shows transverse momentum spectrum of negatively charged hadrons. Experimental data are taken from the STAR Collaboration [17]. Our result well reproduces the experimental data. We display the transverse mass spectra of identified negative charged hadrons (π^-, K^-, p) in Fig. 5. Preliminary experimental data are from the STAR Collaboration [18]. All slopes of the spectra are well reproduced by our calculation. Note that our result of pions and kaons in this figure are rescaled of factor 0.67 for the better fit to the data. The artificial factor 0.67 is chosen by hand here but this number is also consistent with the present experimental results. Because, according to our estimation based on the figure, the both total pions and total kaons in the m_T distribution are less than the ones in the k_T distribution and pseudorapidity distribution as factor about 0.7. Antiprotons is also scaled factor 4.1 in Fig. 5 but only for the clear comparison with the slope. Hence, our calculation successfully reproduces pions and kaons in the pseudorapidity, k_T , and m_T distributions consistently. But as concerns antiprotons, our hydrodynamical model fail to give enough number of antiprotons to reproduce experimental results. We also show the proton spectrum in Fig. 5 for comparison. Figure 6 shows antiproton to proton ratio as a function of rapidity. Experimental data are taken from the BRAHMS Collaboration [19]. Our result shows excellent agreement with the experimental data. However, the numbers of protons and antiprotons will not be reproduced as in Fig. 5. Though we here assume the same freeze-out condition for all particle species, the discrepancy may indicate the more complicated mechanism.

For example, a simple statistical thermal model calculation suggests chemical freeze-out [20] where the numbers of protons and antiprotons are determined by higher chemical freeze-out temperature rather than kinetic freeze-out temperature. For the definite conclusion we need more and more detailed data and much further phenomenological investigation. From the parameter set in Table I, we can see that the energy density is not extremely high but sufficient for the QGP production. The value 2.45 GeV/fm³ which corresponds to the temperature of 178 MeV is only 11% higher than SPS [21]. Large collision energy at RHIC leads to very large volume of the hot matter. Longitudinal extension parameter (≈ 1.6) is about 2.5 times larger than the one of SPS [21]. Initial energy density itself depends strongly on the initial time t_0 which corresponds to longitudinal extension. So much higher energy density should be obtained if we assume an earlier thermalization time. Furthermore, we do not include the thickness of incident nucleon but use almost at profile with gaussian smearing for the transverse direction (see Fig. 2). Hence, maximum energy density of our model is smaller than other models which take the thickness into account [3, 5, 6]. We display the outputs from the uid in Table II. We can see that net baryon number is much smaller than total baryon number of incident nuclei. h_B means average of the chemical potential on the whole freeze-out hypersurface. $h_{T,i}$ is the average transverse velocity of the uid element in $j \in [0, 1]$ at the freeze-out. Lifetimes of the each phase are also shown in Table II. We can see the short lifetime of QGP which reflects the initial maximum energy density is not extremely high. Temperature and chemical potential profile functions are also shown in Fig. 7. The temperature profile function is similar to baryon-free case [22]. The chemical potential profile function tells us that the high temperature uid has small net baryon number. Further discussions including the comparison with the SPS result will be given in Ref. [21].

The two-particle correlation function for chaotic source is calculated through

$$C_2(q; K) = 1 + \frac{I(q; K)}{I(0; k_1)I(0; k_2)} \quad (3)$$

where $K = (k_1 + k_2)/2$, $q = k_1 - k_2$, respectively [23, 24]. We put

$$I(q; K) = K_d(x) \int_0^p \frac{f(k_1; x)f(k_2; x)}{e^{iq \cdot x}} \quad (4)$$

so that $I(0; K)$ reduces to the Cooper-Frye formula with $f(k; x)$ being the Bose-Einstein distribution function. For simplicity at the first trial, we neglect the contributions from resonance decay. Figure 8 shows the projected correlation functions for π^+ with $\eta \in [0.5, 0.125 < K_T < 0.225 \text{ GeV}/c]$. Experimental data are taken from the STAR Collaboration [25]. In each correlation function, our results are corrected by a unique factor whose value is 0.5. The other origin of the reduction is integration with respect to other components of

ture and net baryon number distribution. η stands for the coordinate of the uid, the space-time rapidity. η denotes pseudorapidity only in the figures of particle distribution.

² It is well known that the Cooper-Frye formula has an ambiguity in the treatment of the time-like hypersurface. For example, see Ref. [9, 10, 11, 12, 13].

the relative momenta over the range $0 < q_i < 35 \text{ MeV}/c$. We can see excellent agreements with the experiment as concerns outward and longitudinal direction despite the neglection of resonance contribution. However, sideward correlation function (middle of Fig. 8) is slightly different from the experiment at low q_{side} . This point can be improved by resonance decay. Finally, we compare pair transverse mass $M_T = \sqrt{K_T^2 + m^2}$ dependence of the HBT radii extracted from the fit to the three-dimensional correlation function (4) with the gaussian fitting function

$$C_{2,t}(K; q) = 1 + \exp \left[\frac{R_{\text{out}}^2(K) q_{\text{out}}^2}{R_{\text{side}}^2(K) q_{\text{side}}^2 + R_{\text{long}}^2(K) q_{\text{long}}^2} \right] \quad (5)$$

The results are shown in Fig. 9. As for the longitudinal HBT radii, our result show an excellent agreement with the data both qualitatively and quantitatively. This result indicates the existence of the strong hydrodynamical expansion in the longitudinal direction, which is characteristic to the hydrodynamical model. Sideward HBT radii show qualitative agreement though our results are slightly smaller than the experimental one. That can be seen from the behavior of the sideward correlation function since the HBT radius is related to the width of the correlation function. At the lowest transverse mass, the outward HBT radius is consistent with the experiment. However, the discrepancy between our results and the experimental data appears at the higher transverse mass. Our results decrease with M_T after increase up to $M_T = 0.3 \text{ GeV}/c^2$ while the experimental data show monotonous decrease. As a result, our outward HBT radius is about 2 fm larger than the experiment at $M_T = 0.4 \text{ GeV}/c^2$. Since the sideward HBT radius which stands for the transverse source size shows underestimation, the discrepancy should be due to the time duration. A naive interpretation of the experimental result is that high M_T pions come from high temperature source and the experimental results indicate short lifetime of the high temperature region. On the other hand,

if freeze-out of the system is similar to our model, i.e., freeze-out from 3-dimensional hypersurface, the experimental data suggest very short freeze-out duration or opaque source [26]. Our model shows opaque property due to flow [22] but freeze-out time duration is about 7 fm/c which is larger than the case at SPS. More detailed investigation will be needed for this problem.

In summary, we present a hydrodynamical model calculation for the 130 GeV/nucleon Au+Au collisions data from the RHIC experiment. Our calculation well reproduces the experimental result. The numerical solution indicates that the produced quark-gluon plasma in the RHIC has much lower baryon density, slightly higher energy density, and several times larger extension in the longitudinal direction than in the SPS case, if we compare at the same initial time, $t_0 = 1 \text{ fm}/c$. We present the first analysis of the pion Bose-Einstein correlation data at RHIC based on the hydrodynamical model which takes into account both longitudinal and transverse expansion appropriately. The result is consistent with the experimental data for the most part. In this work, we concentrate our discussion on the RHIC data. More detailed discussion including the comparison with the SPS data will be given in the forthcoming paper [21].

Acknowledgments

The authors are much indebted to Professor I. Ohba and Professor H. Nakazato for their fruitful comments. They also would like to thank Dr. H. Nakamura and other members of high energy physics group at Waseda University for helpful discussions. One of the authors (C.N.) would like to acknowledge the financial support by the Soryushi Shogakukan. This work is partially supported by Waseda University Grant for Special Research Projects No 2001A-888 and Waseda University Media Network Center.

[1] Quark Matter 2001, to be published in the proceedings of the Fifteenth International conference on Ultra-Relativistic Nucleus-Nucleus Collisions. (Stony Brook, USA, January 14-21, 2001).

[2] T. Ishii and S. Muroya, Phys. Rev. D 46, 5156 (1992).

[3] P. F. Kolb, P. Huovinen, U. Heinz, and H. Heiselberg, Phys. Lett. B 500, 232 (2001).

[4] J. D. Bjorken, Phys. Rev. D 27, 140 (1983).

[5] D. Zschiesche, S. Schramm, H. Stocker, and W. Greiner, nucl-th/0107037.

[6] T. Hirano, nucl-th/0108004.

[7] C. Nonaka, E. Honda, and S. Muroya, Eur. Phys. J. C 17, 663 (2000).

[8] F. Cooper and G. Frye, Phys. Rev. D 10, 186 (1974).

[9] Y. M. Sinyukov, Z. Phys. C 43, 401 (1989).

[10] M. I. Gorenstein and Y. M. Sinyukov, Phys. Lett. 142B, 425 (1984).

[11] F. Grossi, Y. Hamamoto, and T. Kodama, Phys. Lett. B 355, 9 (1995).

[12] K. A. Bugaev, Nucl. Phys. A 606, 559 (1996).

[13] H. Heiselberg, Heavy Ion Phys. 5, 1 (1997).

[14] J. Sollfrank, P. Koch, and U. Heinz, Z. Phys. C 52, 593 (1991).

[15] T. Hirano, Phys. Rev. Lett. 86, 2754 (2001); T. Hirano, K. Tsuchiya, and K. Kamoto, nucl-th/0011087.

[16] A. Wosman et al. (PHOBOS Collaboration), in the proceedings for Quark Matter 2001, to be published in Nucl. Phys.

[17] C. Adler et al. (STAR Collaboration), Phys. Rev. Lett. 87, 112303 (2001).

[18] J. W. Harris et al. (STAR Collaboration), in the proceedings for Quark Matter 2001, to be published in Nucl.

Phys.

[19] I. G. Bearden et al. (BRAHMS Collaboration), Phys. Rev. Lett. 87, 112305 (2001).

[20] J. Cleymans and K. Redlich, Phys. Rev. Lett. 81, 5284 (1998); see also P. Braun-Munziger, D. M. Agestro, K. Redlich, and J. Stachel, hep-ph/0105229, for the analysis of RHIC data.

[21] T. Hirano, K. Morita, S. Muroya, and C. Nonaka, in preparation.

[22] K. Morita, S. Muroya, H. Nakamura, and C. Nonaka, Phys. Rev. C 61, 034904 (2000).

[23] E. V. Shuryak, Phys. Lett. 44B, 387 (1973).

[24] Y. Hamamoto and S. S. Padula, Phys. Rev. D 37, 3237 (1988).

[25] C. Adler et al. (STAR Collaboration), Phys. Rev. Lett. 87, 082301 (2001).

[26] H. Heiselberg and A. P. Vischer, Eur. Phys. J. C 1, 593 (1998).

Figures

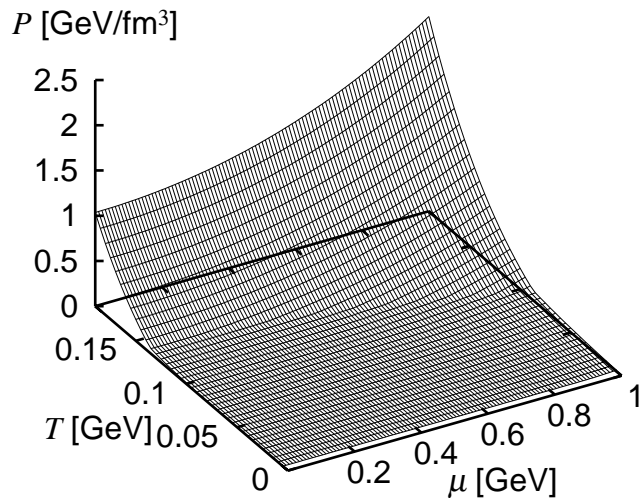


FIG. 1: Pressure as a function of temperature and chemical potential.

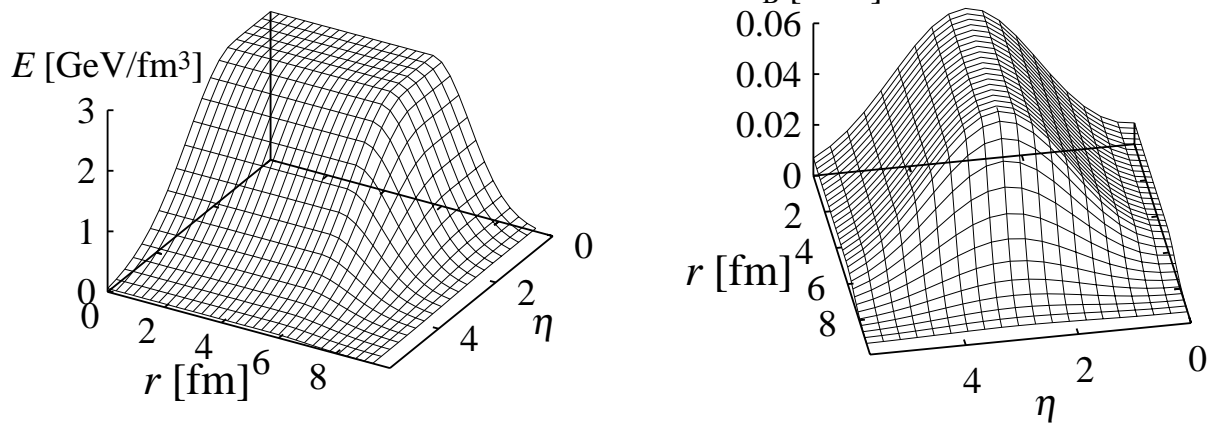


FIG. 2: Initial energy density (left) and net baryon number density (right) distribution.

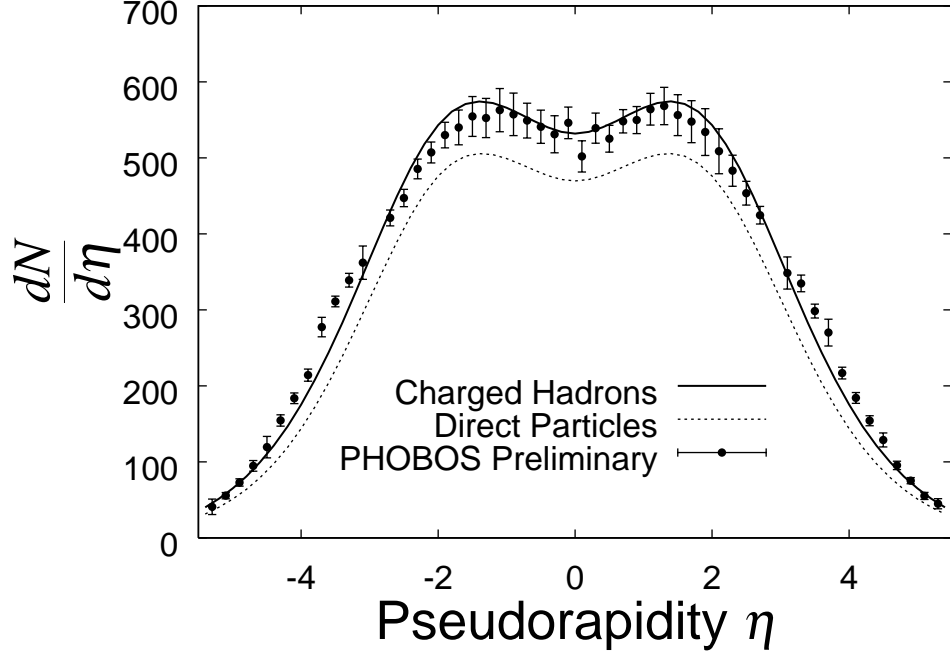


FIG. 3: Pseudorapidity distribution of charged hadrons. Solid line shows our result ($\pi; K; p$) including resonance contribution. Dotted line denotes contribution of the directly emitted particles from the freeze-out hypersurface. Closed circles are preliminary result from the PHOBOS Collaboration [16].

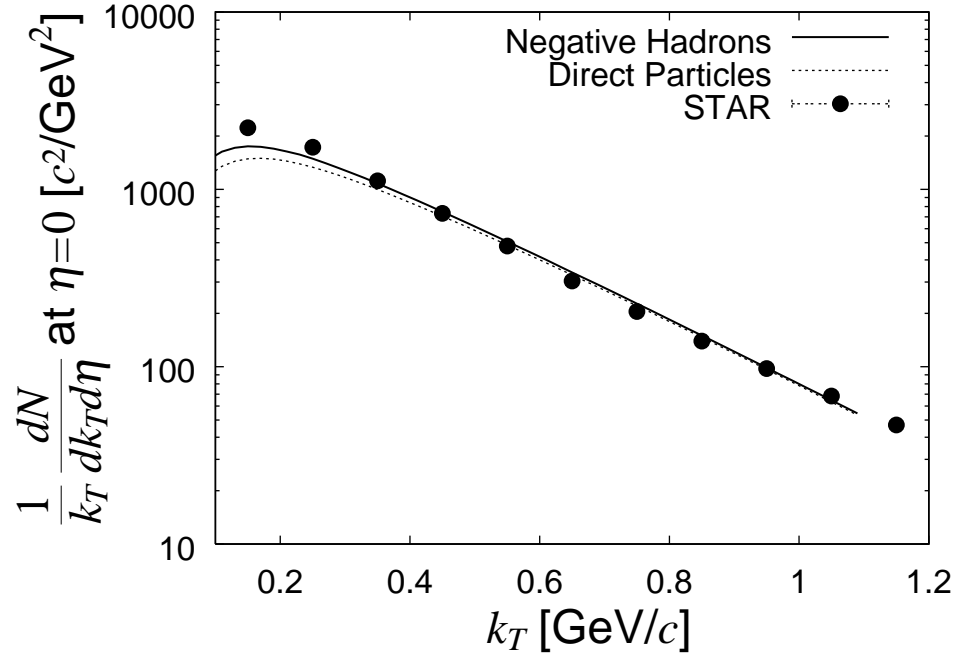


FIG. 4: Transverse momentum spectrum of negatively charged hadrons. As in Fig. 3, solid line and dotted line show total number of particles and directly emitted particles from the freeze-out hypersurface, respectively. Closed circles are data from the STAR Collaboration [17].

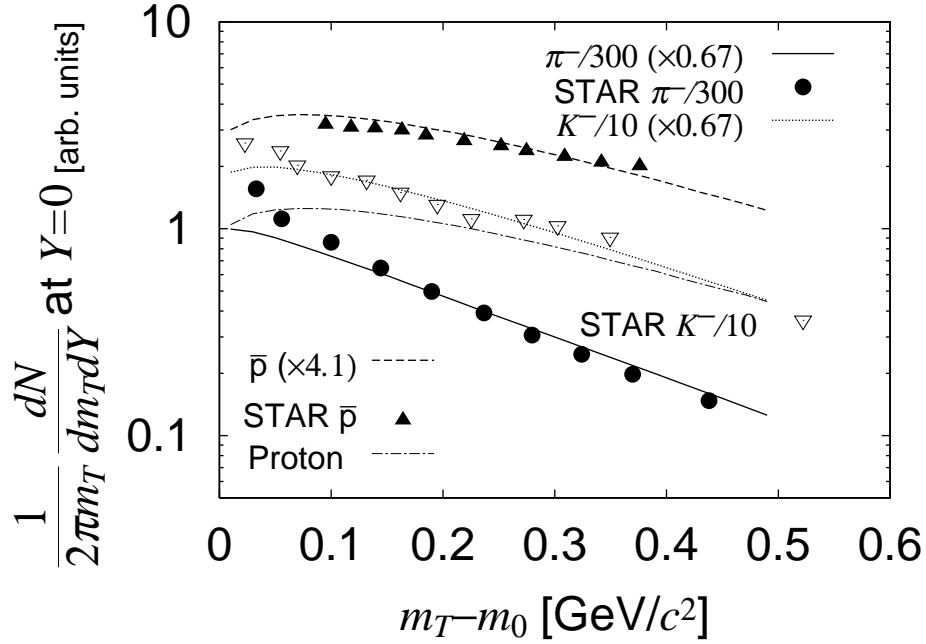


FIG. 5: Transverse mass spectra of negatively charged hadrons. Solid line, dotted line and dashed line denote π^- , K^- and p yield of our result. Each line is rescaled by some factors, see text for details. Closed circles, open triangles and closed triangles are preliminary data from the STAR Collaboration [18]. Dash-dotted line shows proton yield of our calculation for comparison.

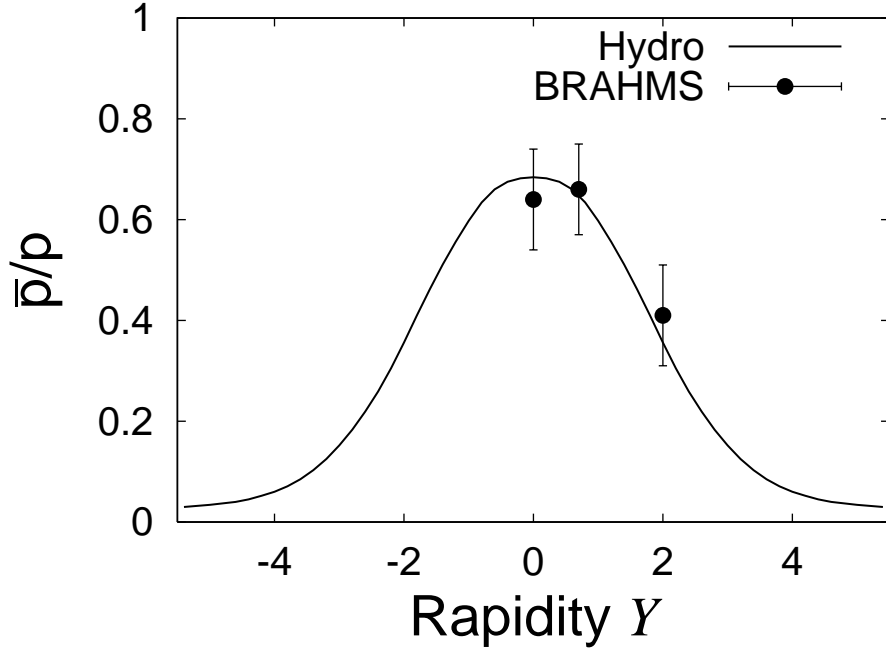


FIG. 6: Rapidity dependence of anti-proton to proton ratio. Experimental data are taken from the BRAHMS Collaboration [19].

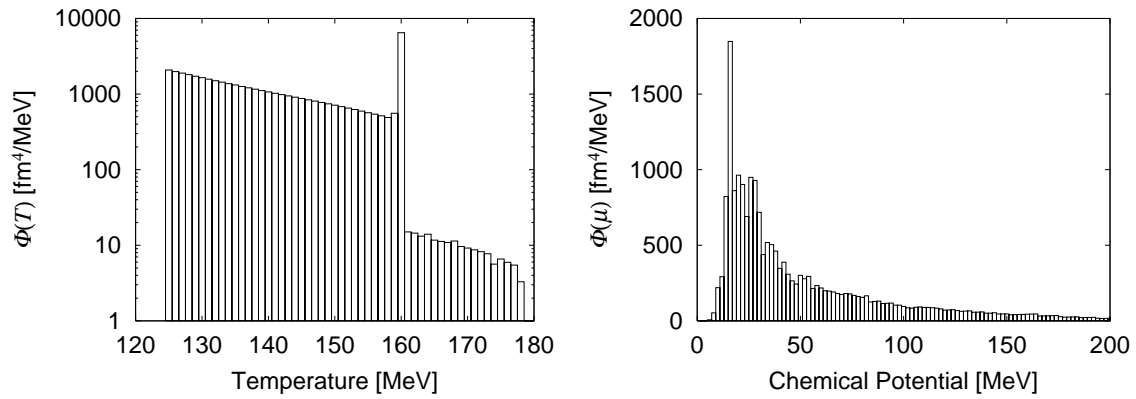


FIG. 7: Temperature (left) and chemical potential (right) profile functions.

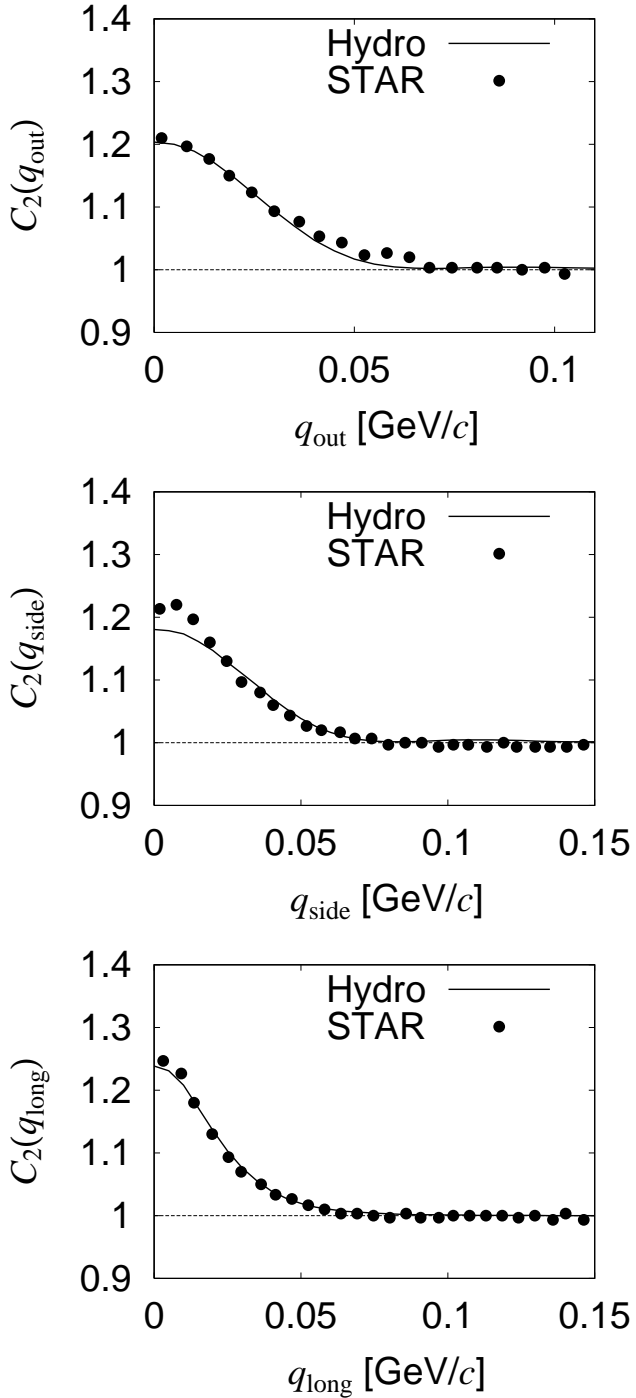


FIG. 8: Two-particle Bose-Einstein correlation functions for π^+ . Top, middle and bottom figures show outward, sideward and longitudinal correlation functions, respectively. In each figure, correlation function is integrated with respect to other two components from 0 to 35 MeV/c . Experimental data (closed circles) are taken from the STAR Collaboration [25].

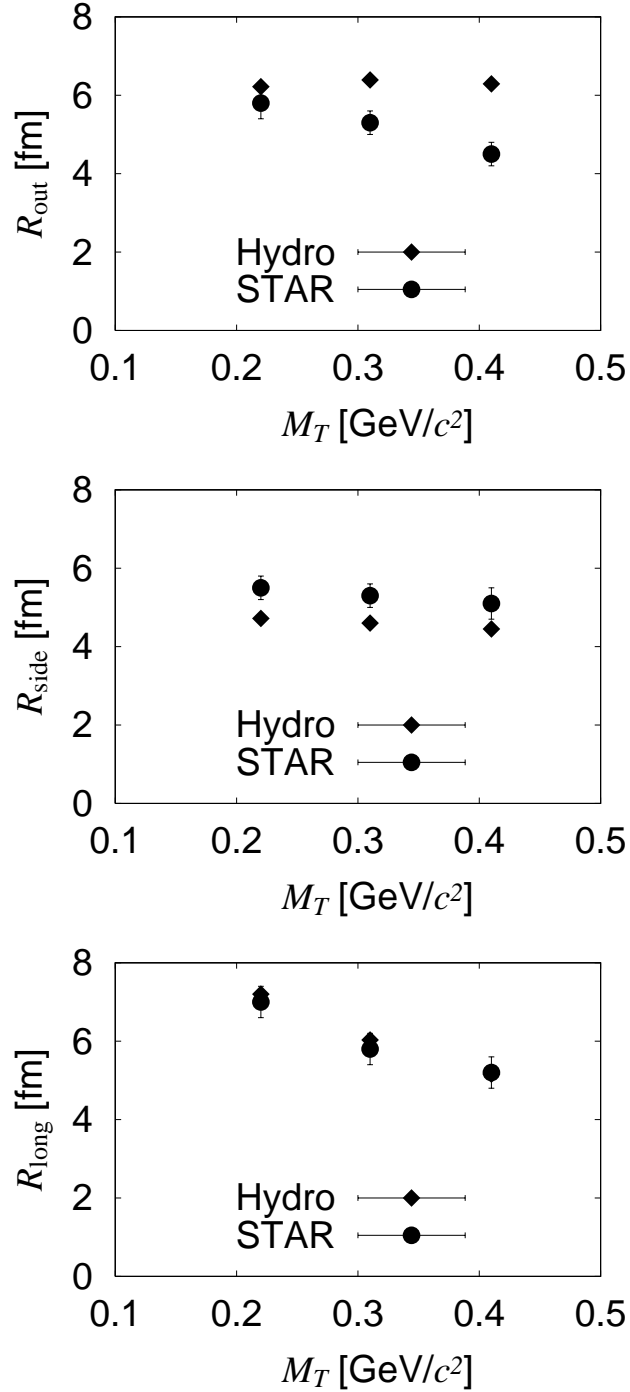


FIG. 9: M_T dependence of HBT radii. Top, middle and bottom figures correspond to outward, sideward and longitudinal HBT radii, respectively. Experimental data (closed circles) are taken from the STAR Collaboration [25].

Tables

TABLE I: Parameter set for the Au+Au collisions.

| | |
|---|--------------------------|
| Maximum initial energy density E_0 | 2.45 GeV/fm ³ |
| Maximum initial net baryon density n_{B0} | 0.06 fm ⁻³ |
| Longitudinal gaussian width σ_L of initial energy density | 1.6 |
| Longitudinal extension σ_L of the π region in the initial energy density | 1.3 |
| Longitudinal gaussian width σ_L of the initial net baryon density | 1.3 |
| Space-time rapidity η at maximum of the initial net baryon distribution | 3.0 |
| Gaussian smearing parameter r of the transverse profile | 1.3 |
| Freeze-out temperature T_f | 125 MeV |

TABLE II: Output.

| | |
|---|------------|
| Net baryon number | 65 |
| Mean chemical potential at freeze-out μ_B | 74.7 MeV |
| Mean transverse flow velocity v_T of the uid at $j < 0.1$ | 0.367c |
| Lifetime of the QGP phase τ_{QGP} | 1.38 fm/c |
| Lifetime of the mixed phase τ_{mixed} | 6.27 fm/c |
| Total lifetime of the uid τ_{HAD} | 15.43 fm/c |